AIP | Review of Scientific Instruments

Characterization of a cesium surface ionization source with a porous tungsten ionizer. I

G. D. Alton

Citation: Rev. Sci. Instrum. **59**, 1039 (1988); doi: 10.1063/1.1139776
View online: http://dx.doi.org/10.1063/1.1139776
View Table of Contents: http://rsi.aip.org/resource/1/RSINAK/v59/i7
Published by the American Institute of Physics.

Characterization of a cesium surface ionization source with a porous tungsten ionizer. I

G. D. Alton

Oak Ridge National Laboratory, P. O. Box X, Building 6000, Oak Ridge, Tennessee 37831

(Received 22 October 1987; accepted for publication 8 March 1988)

A cesium surface ionization source of the type and geometry customarily used in conjunction with sputter-type negative heavy ion sources has been characterized. Measurements have been made of positive-ion production and probabilities of ionization as functions of extraction voltage and cesium oven temperature for ionizer porosities of 0.7 and 0.8. The perveance P of the source, when operated in the space-charge-limited regime with the $\rho = 0.7\rho_0$ ionizer, is found from experiment to be $7.61 \times 10^{-4}\,\mu$P, while that for the $\rho = 0.8\rho_0$ ionizer is $1.92 \times 10^{-4}\,\mu$P. These values are lower by factors of 3.88 and 15.53, respectively, than those predicted by numerical solution to Poisson's equation for full area emission from the source. Positive-ion current versus ionizer temperature data are also presented along with mechanical design features of the source.

INTRODUCTION

Surface ionization sources of the porous tungsten ionizer variety are used extensively as integral parts of negative heavy ion sources as well as in positive-ion-source applications. For negative-ion-source applications, the surface ionization source is used to generate positive-ion beams from a Group-IA element such as cesium for sputtering a sample containing the material of interest. The presence of an electropositive material such as cesium or other Group-IA elements in or on the sample surface greatly enhances the probability of negative-ion formation during the sputtering process.[1] Negative-ion sources, based on this principle, have taken a variety of forms including the original cone geometry source[2] and variations thereof,[3,4] an oblique incidence source,[5] and inverted geometry negative-ion sources.[6,7] Many of these sources have been superseded by more recent developments such as described in Refs. 10–13. For a more comprehensive review of these and other negative-ion-source developments, the reader is referred to the literature cited in Refs. 8–14.

Several types of surface ionization sources have been developed for positive-ion generation. The source type is characterized by the means by which the atomic vapor is fed onto the ionizing surface as well as the method used to extract ions from the source. Perhaps, the most highly developed and, in many respects, the simplest type of surface ionization source is the porous ionizer type which utilizes an ionizer made of sintered tungsten. In this type of source, the atomic vapor is fed from an oven through a sealed tube to the ionizer surface. Some of the atoms which strike the inner surface are trapped by the surface and are subsequently diffused through the thin porous tungsten ionizer where they are evaporated in neutral or ionic form. The source is especially suitable for the alkali metals (Cs, Rb, and K), which have high vapor pressures and relatively low critical temperatures—the temperature required to evaporate the material in ionic form. This type of ion source has also been highly developed for possible ion propulsion applications.[15] Surface ionization sources for the generation of Li^+ or Na^+ (Ref. 16), and In^+ (Ref. 17) ions have also been developed and characterized. The tungsten ionizer frequently used in these sources typically has a density of $\sim 80\%$ that of solid tungsten.

Although negative-ion yields, emittances, operational parameters, and ion optics have been documented for many negative-ion sources which utilize cesium surface ionization sources, little information is presently available concerning the surface ionization source itself. For example, information concerning the positive cesium ion generation capabilities of the source in terms of source operational parameters is not generally available; also, the dependence of positive-ion current on ionizer porosity has not been reported in the literature. The need for such information was the motivating factor which led to the present investigations.

The surface ionization source described in this article is similar in design to that used by Middleton and Adams[2] in the original cone geometry negative-ion source; both sources are, in turn, similar in principle to the sources described in Refs. 16 and 17. A companion report, designated as Part II,[18] deals with negative-ion generation in the refocus-type negative-ion source[3,4] equipped with a cesium surface ionization source such as the one described in this report.

I. THE SURFACE IONIZATION MECHANISM

Positive or negative ions of several elements and molecules can be produced by surface ionization. A particle of low ionization potential I_i can be ionized by contact with a surface of high work function ϕ that is hot enough to thermally evaporate the particle in ionic form. In this process, a valence electron of the adsorbed atom or molecule is lost to the surface upon evaporation or desorption of the positive ion. The most easily ionized materials for which the technique can be effected are the alkali metals (Cs, Rb, K, Na, and Li). The alkaline-earth, rare-earth, and transuranic ele-

 0034-6748/88/071039-06$01.30

ments can also be formed as positive ions through the process but with lower efficiencies. The elements with high heats of vaporization or high ionization potentials are the most difficult to ionize.

When an atom is near or adsorbed on a hot surface, the valence level is broadened. Furthermore, electrons in a hot metal possess a Fermi distribution of energies, and thus when the valence level of the adsorbed atom is sufficiently broadened, electrons can move to the metal from the atom and from the metal to the atom. The probability for arrival of a particle at a position far from the metal surface in a given state depends on the difference between the work function ϕ of the metal and the first ionization potential I_i of the absorbed atom. For thermodynamic equilibrium processes, the ratio of ions to neutrals that leave an ideal surface can be predicted from Langmuir–Saha surface ionization theory. For atoms or molecules leaving a heated surface, the probability of positive-ion formation P_i is given by

$$P_i = \frac{\omega_+}{\omega_0}\left(\frac{1-r_+}{1-r_0}\right)\exp\left(\frac{\phi - I_i}{kT}\right) \times\left[1+\frac{\omega_+}{\omega_0}\left(\frac{1-r_+}{1-r_0}\right)\exp\left(\frac{\phi - I_i}{kT}\right)\right]^{-1}, \quad (1)$$

where r_+ and r_0 are the reflection coefficients of the positive and neutral particles at the surface, ω_+ and ω_0 are statistical weighting factors, T is the absolute temperature, and k is Boltzmann's constant. Optimum-ionization efficiencies are obtained for high work function materials and low ionization potential atomic species. For elements for which $I_i > \phi$, the process is much less efficient. For example, the work function for clean tungsten is about 4.6 eV and the ionization potential for indium is 5.8 eV. Thus, in this case, the exponential term $(\phi - I_i)$ in the Langmuir–Saha relation is negative and, therefore, the probability of ionization is low. A particular technique that helps to improve the ionization efficiency is to incorporate an oxygen spray that is directed onto the ionizer surface. This increases the work function of the emitting surface and, hence, the efficiency of ionization. The probability of ionization predicted by Eq. (1) assumes that the ions are extracted as fast as they are formed and thus is not valid whenever space-charge effects are present.

II. SOURCE DESCRIPTION

The ion source, shown in Fig. 1, was developed at the Oak Ridge National Laboratory for use in a cone geometry negative-ion source.[2] The source consists of a cesium reservoir, a removable ionizer tube assembly, and a housing for mounting the ionizer heater and heat shielding to which is attached the focus electrode. With the exception of portions of the ionizer tube assembly, ionizer heater, heat shielding, and electrical feedthroughs, the unit is constructed from 300 series stainless steel.

The extraction electrode system. The electrode system is based on the well-known Pierce geometry design.[19] The optical characteristics of the source were carefully studied by numerical solution to Poisson's equation with various degrees of space charge present. Examples of the effect of space charge on a 30-keV ion beam accelerated through the electrode system are shown in Fig. 2. These studies reveal that the perveance P of the source when operated in the space-charge-limited regime for full area cesium extraction and an electrode spacing of 1 cm is $2.95\times10^{-3}\,\mu$P (1 P $= 10^6\,\mu$P), where P is defined by the following equation:

$$I^+(\text{mA}) = 10^3 P V_{\text{ex}}^{3/2} \quad (2)$$

where I^+ is the positive-ion current and V_{ex} (in volts) is the extraction potential.

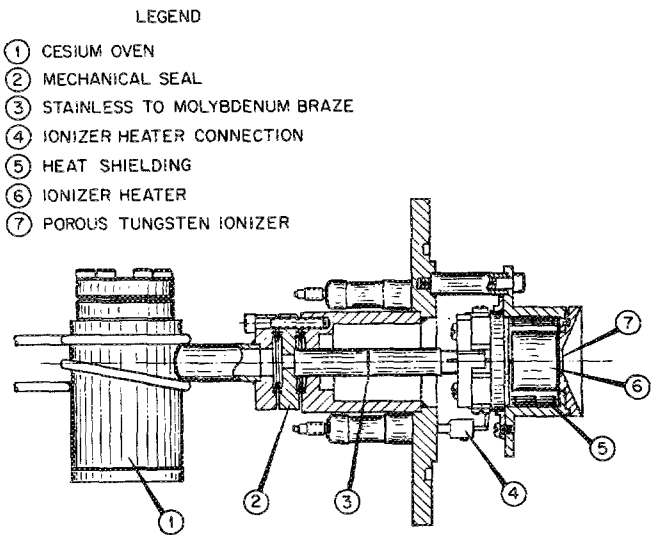

FIG. 1. The cesium surface ionization source.

The cesium reservoir (oven). The cesium reservoir (oven) is heated by a commercially available,[20] band-type 115-V ac, 175-W heater which slips around the reservoir. As shown in Fig. 3, an approximately linear relationship exists between heater current and equilibrium temperature of the reservoir. All measurements were made with a Chromel–Alumel thermocouple clamped in intimate contact with the cesium reservoir; three-ply aluminum foil heat shielding is placed around the reservoir. We note differences in the pow-

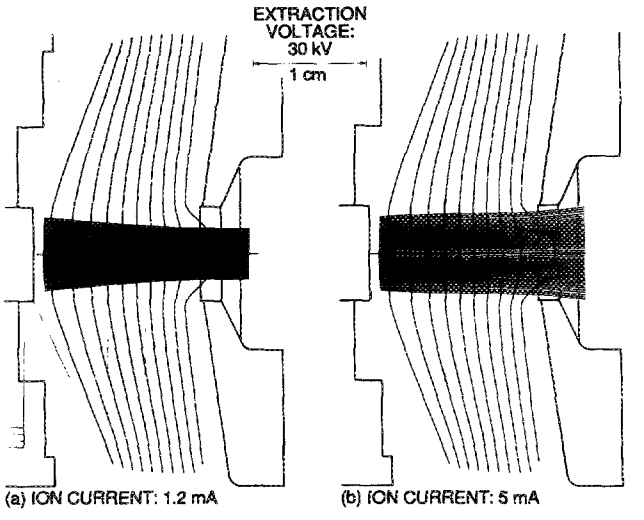

FIG. 2. Calculated space-charge effects in the cesium-ion extraction region of the surface ionization source.

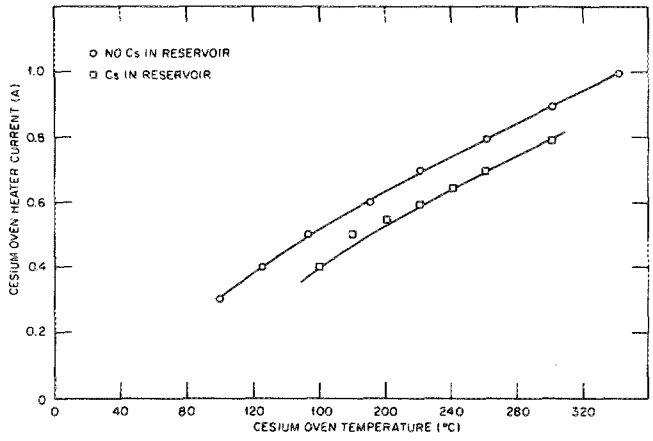

FIG. 3. Relationship between heater current and cesium oven temperature with and without cesium in the reservoir. The increase in reservoir temperature at a given heater current is attributable to the so-called "heat pipe" effect where energy transferred from the ionizer to cesium particles impinging on the hot tungsten surface is conducted back through the cesium vapor to the reservoir.

er required to maintain a given oven temperature with and without cesium in the oven. This behavior is attributable to the so-called heat pipe effect where heat is conducted from the hot ionizer ($\sim$1100 °C) to the reservoir through the vapor medium.

The cesium vapor pressure versus cesium oven temperature. The vapor pressure p of liquid cesium within the reservoir and tube assembly can be expressed in terms of the reservoir temperature T by the following approximation:

$$p(\text{Torr}) = \frac{10(11.0531 - 4041/T)}{T^{1.35}}, \tag{3}$$

where p has units of Torr and T is expressed as absolute temperature (K). Equation (3) was deduced from the cesium vapor pressure data of Langmuir and Taylor[21] by Nesmeyanov.[22]

The ionizer tube assembly. The ionizer tube assembly consists of a molybdenum tube which is brazed with Au–Ni alloy into a double-sided metal-to-metal vacuum flange which effects seals between the cesium reservoir and tube assembly and between the tube and vacuum housing. The ionizer is a porous tungsten frit[23] 1 mm in thickness and 6.25 mm in diameter; the porosity P_r is defined in terms of the ratio of the density of the frit ρ to the solid density ρ_0 of $P_r = \rho/\rho_0$, where P_r is usually 0.8. The tungsten frit is fusion bonded to the end of the molybdenum tube by electron beam heating. The ionizer is maintained in temperature by means of a cylindrical heater which surrounds the end of the molybdenum tube. The heating element of the ionizer heater is made of 1.25-mm-diam, 97% W/3% Re, alloy wire with a typical room-temperature resistance of 22 mΩ.[23] The wire is embedded in a sintered Al_2O_3 matrix, which is enclosed in a molybdenum cylindrical housing of length 18.75 mm and outer diameter 21.88 mm; the inner bore of the heater is 8 mm. The heater is surrounded by three layers of tantalum heat shielding.

The required operating temperature of the ionizer was determined by measuring the negative-ion yield produced in a modified refocus geometry cone source[24] as a function of the ionizer current. The ionizer temperature was subsequently measured by inserting a conventional Chromel–Alumel thermocouple through the cesium oven and ionizer tube until contact was made with the ionizer frit surface. The correlation between relative negative-ion yield and ionizer temperature was then made (Fig. 4). As noted, the negative-ion current turns on very abruptly above the critical temperature ($\sim$1000 °C), the temperature required to evaporate cesium ions from the hot surface. At high temperatures, the negative-ion yield begins to decrease, probably due to a reduction in the mean residence time for atomic cesium on the surface, i.e., a cesium atom must reside on the surface long enough to reach thermodynamic equilibrium for ionization to take place. In order to avoid large changes in beam current due to small changes in power, it is desirable to operate the ionizer a few degrees higher than the onset value (usually 1100 °C).

Estimation of the cesium flux striking the ionizer surface. The ionizer is customarily operated at a fixed temperature of $\sim$1100 °C, so that the diffusion rate through the ionizer is governed by the rate of arrival and probability of trapping of the impinging neutral vapor on the internal ionizer surface, and the rate of evaporation at the emission surface. The number of particles striking per unit area dA per unit time dt is given by the familiar relation

$$\frac{dN}{dA\,dt} = \frac{n\bar{v}}{4}, \tag{4}$$

where $\bar{v}$ is the average velocity of a cesium atom within the cesium reservoir/ionizer tube chamber at temperature T and n is the number of particles per unit volume within the chamber.

A portion of the flux impinging on the reservoir side of the ionizer will be captured by the porous surface and may be subsequently diffused through the frit to the extraction side of the ionizer where the cesium particles can be evaporated either as ions or neutrals. The number of captured particles, thus, will be given by

$$\frac{dN}{dA\,dt} = \frac{n\bar{v}}{4} P_c, \tag{5}$$

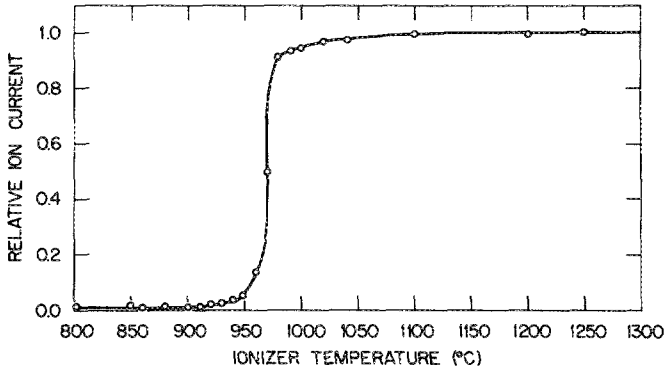

FIG. 4. Relative negative-ion current vs ionizer temperature for the cesium surface ionization source shown in Fig. 1. The temperature at which the cesium surface ionization process abruptly turns on is referred to as the critical temperature for the ionization of cesium on hot tungsten.

where P_c represents the probability for capture at the interior surface.

Inserting values for n in terms of vapor pressure p from Eq. (3) for p in dyn/cm^2 and $\bar{v}$ from the kinetic theory of gases into Eq. (5), we obtain an expression for the number of particles striking the frit per unit area per unit time which are captured

$$\frac{dN}{dA\,dt} = \frac{1}{2}\left(\frac{2}{k\pi M}\right)^{1/2} \frac{1.33\times 10^3}{T^{1.85}} \times 10\left(11.0531 - \frac{4041}{T}\right) P_c. \quad (6)$$

III. POSITIVE-ION GENERATION AND PROBABILITY OF CESIUM IONIZATION CHARACTERISTICS OF THE SOURCE

The positive-ion generation capabilities of the source were examined for each of two new ionizers with porosities, P_r of 0.7 and 0.8. A modified refocus-type negative-ion source[24] was used for these measurements; the experimental arrangement is shown in Fig. 5. Positive ions extracted from the source were focused into a biased and shielded Faraday cup located immediately behind the sample indexing mechanism of the source by means of the conventional lens/steering assembly associated with the negative-ion source. The results of these measurements are displayed in Figs. 6 and 7 for the $\rho = 0.7\rho_0$ and $\rho = 0.8\rho_0$ ionizers, respectively. Numerically computed space-charge-limited ion current versus extraction voltage values are also shown for comparison. The computed space-charge-limited relation was scaled to the high cesium oven temperature curve at an extraction voltage V_{ex} of 12 kV which appears to be within the space-charge-limited flow region of the source. The perveance P of the source, determined by numerical solution of Poisson's equation for an emitting area A_0, equivalent to the full area of the ionizer surface ($A_0 = 0.32$ cm^2), was found to be $2.95\times 10^{-3}\,\mu$P.

Scaling factors required to adjust the Langmuir–Child relation to the high-temperature experimental data in the space-charge-limited regime of the source at a particular extraction voltage $V_{ex} = 12$ kV were determined and perveances P and effective emitting areas A_{eff} computed for each of the two ionizers. (The extraction electrode gap d was assumed to be fixed at 1 cm.) The perveances for cesium ions of the two sources were found to be

$$P = 7.61\times 10^{-4}\,u\text{P}, \quad \rho = 0.7\rho_0$$

and

$$P = 1.92\times 10^{-4}\,\mu\text{P}, \quad \rho = 0.8\rho_0.$$

The corresponding areas of the ionizers were found to be

$$A_{eff} = 0.258A_0, \quad \rho = 0.7\rho_0$$

and

$$A_{eff} = 0.064A_0, \quad \rho = 0.8\rho_0,$$

where A_0 is the full area of the ionizer surface.

Returning to discussions of the data displayed in Figs. 6 and 7, several points are worthy of mention. First of all, we note that the region over which space-charge-limited flow holds increases with cesium oven temperature and extraction voltage. Each data set spans a region of space-charge-limited flow, a transition region and the onset of the temperature-limited region of the source. The spacing between adjacent curves for the temperature-limited condition suggests the following simple relationships between the ion current and cesium oven temperature for the two ionizers:

$$I^+(\text{mA}) = 3.34\times 10^{-2}T(\text{K}) - 14.71, \quad \rho = 0.7\rho_0 \quad (7)$$

and

$$I^+(\text{mA}) = 6.53\times 10^{-3}T(\text{K}) - 2.99, \quad \rho = 0.8\rho_0. \quad (8)$$

These expressions, in turn, can be correlated with total particle emission at the surface:

$$\frac{dN}{dt} = 2.09\times 10^{14}T(\text{K}) - 9.10\times 10^{16}, \quad \rho = 0.7\rho_0, \quad (9)$$

$$\frac{dN}{dt} = 4.08\times 10^{13}T(\text{K}) - 1.87\times 10^{16}, \quad \rho = 0.8\rho_0. \quad (10)$$

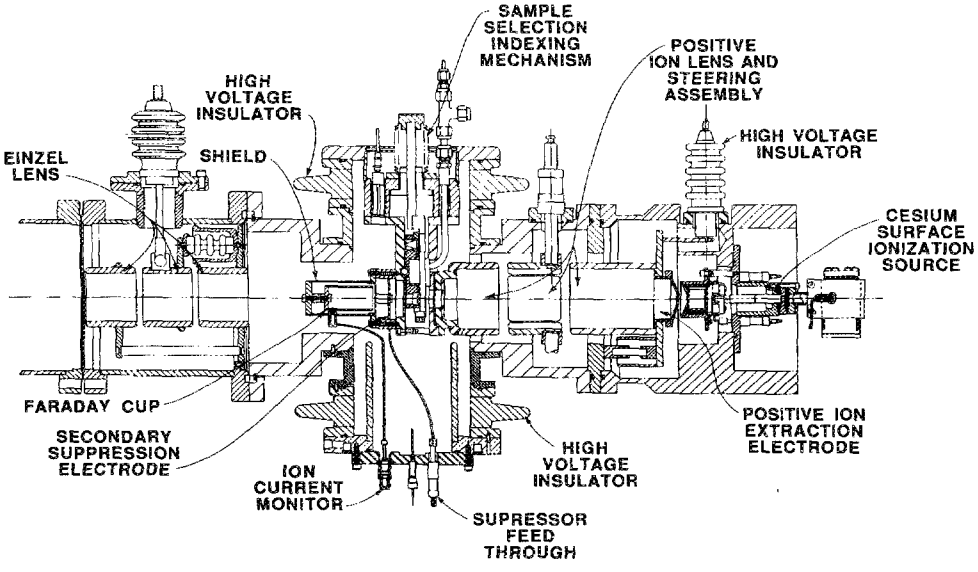

FIG. 5. Experimental arrangement for determining the cesium-ion current I^+ vs extraction voltage V_{ex}. The cesium surface ionization source is mounted on a modified commercially available refocus-type negative-ion source (Ref. 24).

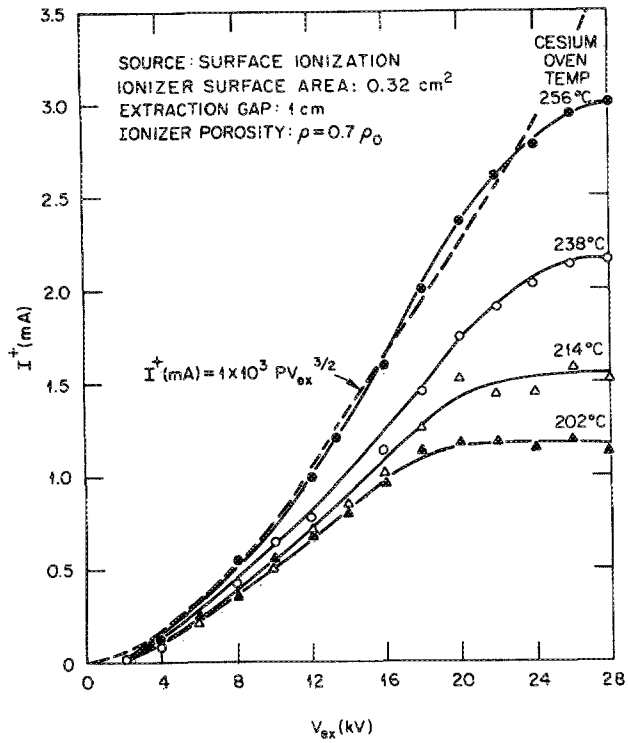

FIG. 6. The cesium-ion current I^+ vs extraction voltage V_{ex} with cesium oven temperature as a parameter for the $\rho = 0.7\rho_0$ ionizer. Also shown for comparison is the numerically computed space-charge limited current vs extraction voltage; the space-charge-limited current was fit to the experimental data at an extraction voltage of 12 keV.

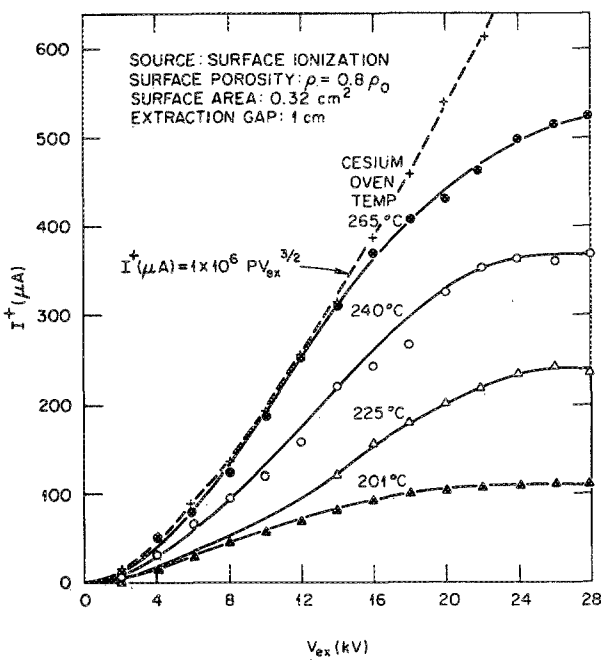

FIG. 7. The cesium-ion current I^+ vs extraction voltage V_{ex} with cesium oven temperature as a parameter for the $\rho = 0.8\rho_0$ ionizer. Also shown for comparison is the numerically computed space-charge-limited current vs extraction voltage; the space-charge-limited current was fit to the experimental data at an extraction voltage of 12 keV.

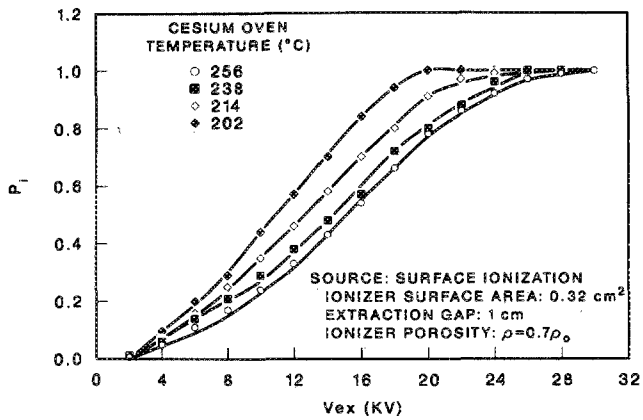

FIG. 8. The probability of cesium surface ionization with the source equipped with a $\rho = 0.7\rho_0$ ionizer. These data illustrate the effect of space charge on the probability for cesium surface ionization.

In terms of the number of particles emitted per cm^2 per second from the total area of the ionizer, these expressions become

$$\frac{dN}{dA\,dt} = 6.53\times10^{14}T(\mathrm{K}) - 2.87\times10^{17}, \quad \rho = 0.7\rho_0 \quad (11)$$

and

$$\frac{dN}{dA\,dt} = 1.28\times10^{14}T(\mathrm{K}) - 5.84\times10^{16}, \quad \rho = 0.8\rho_0. \quad (12)$$

Under steady-state conditions, the rate of capture (trapping) at the interior surface must be equal to the rate of emission at the exterior surface; therefore, the above relations also hold for the capture process. The probability for capture of an impinging particle by the interior surface of the $\rho = 0.7\rho_0$ ionizer can be determined by equating Eqs. (6) and (11) and for the $\rho = 0.8\rho_0$ ionizer, Eqs. (6) and (12).

If we assume that the probability for ionization is unity in the temperature-limited regime (the point at which the cesium-ion current I^+ vs extraction voltage V_{ex} reaches a constant value), then the probability for ionization at any other extraction voltage is just the ratio of the current at the chosen extraction voltage to the temperature-limited current. Using this definition, the probabilities of ionization were determined for both ionizers. Data for the $\rho = 0.7\rho_0$ ionizer are displayed in Fig. 8. These data point out rather dramatically the effect of space charge on the probability for ionization of cesium as it leaves the hot tungsten surface. The space-charge effect, thus, reduces the probability for ionization, even though the Langmuir–Saha relation predicts unit ionization efficiency.

ACKNOWLEDGMENTS

The author is indebted to Gregory Kohring, Oak Ridge Associated Universities Summer Research Participant, who assisted in these experiments and to Jewell Ellis for skillful typing of the manuscript.

This research was sponsored by the Division of Basic Energy Sciences, U.S. Department of Energy, under Contract No. DE-AC05-840R21400 with Martin Marietta Energy Systems, Inc.

[1]V. E. Krohn, Jr., Appl. Phys. **33**, 3523 (1962).
[2]R. Middleton and C. T. Adams, Nucl. Instrum. Methods **122**, 35 (1974).
[3]G. Doucas, H. R. M. Hyder, and A. B. Knox, Oxford Univ. Rep. 19 (1975).
[4]The Hiconex 834 Negative Ion Source, a product of General Ionex Corporation, Ipswich, MA.
[5]G. D. Alton, IEEE Trans. Nucl. Sci. **NS-23**, 1113 (1976).
[6]K. R. Chapman, IEEE Trans. Nucl. Sci. **NS-23**, 1109 (1976).
[7]J. L. Yntema and P. J. Billquist, Nucl. Instrum. Methods, Phys. Res. **220**, 107 (1984).
[8]G. D. Alton, *Applied Atomic Collisions Physics, Vol. 4: Condensed Matter*, edited by H. S. W. Massey, E. W. McDaniel, and B. Bederson (Academic, Orlando, FL, 1983), p. 44.
[10]R. Middleton, Nucl. Instrum. Methods **214**, 139 (1983).
[11]G. D. Alton, Nucl. Instrum. Methods **A244**, 133 (1986).
[12]G. D. Alton and G. D. Mills, IEEE Trans. Nucl. Sci. **NS-32**, 1822 (1985).
[13]G. D. Alton, Proceedings of the Eleventh Symposium on Ion Sources and Ion-Assisted Technology, Tokyo, Japan, 1987, p. 157.
[14]G. D. Alton, Proceedings of the International Ion Beam Engineering Congress, Kyoto, Japan, 1983, Vol. 1, p. 85.
[15]G. R. Brewer, *Ion Propulsion* (Gordon and Breach, New York, 1970).
[16]H. L. Daley and J. Perel, Rev. Sci. Instrum. **42**, 1324 (1971).
[17]H. L. Daley, J. Perel, and R. H. Vernon, Rev. Sci. Instrum. **37**, 473 (1966).
[18]G. D. Alton, Rev. Sci. Instrum. **59**, 1045 (1988) (Paper II; succeeding paper).
[19]J. R. Pierce, *Theory and Design of Electron Beams* (Van Nostrand, New York, 1954), Chap. X, p. 181.
[20]Hot-Watt, Inc., Danvers, MA.
[21]J. B. Taylor and I. Langmuir, Phys. Rev. **51**, 753 (1937).
[22]A. N. Nesmeyanov, *Vapour Pressure of the Elements*, edited and translated by J. I. Carasso (Academic, New York, 1963).
[23]The ionizer frit and heater are products of Spectra-Mat, Inc. of Watsonville, CA.
[24]The Hiconex 834 negative-ion source of Ref. 4 as modified to accommodate the ORNL-designed surface ionization source described in the present report.